Investigation of wide-aperture plasmonic detectors by a tightly focused terahertz beam

D M Yermolaev[1], Ye A Polushkin[1], V E Zemlyakov[1], N A Maleev[2], V V Popov,[3] A V Muravjov[4], S L Rumyantsev[4], M S Shur[4] and S Yu Shapoval[1]

[1]Institute of Microelectronic Technology and High-Purity Materials, Russia
[2]Ioffe Physical Technical Institute, Russia
[3]Kotelnikov Institute of Radio Engineering and Electronics (Saratov Branch), Russia
[4]Rensselaer Polytechnic Institute, USA

E-mail: shapoval@iptm.ru

Abstract. Terahertz response of wide-aperture plasmonic detectors is studied experimentally by using a focused terahertz radiation with frequencies 1.63, 1.89 and 2.55 THz. Two different types of plasmonic detector have been investigated: (i) field-effect transistor (FET) with a grating-gate of large (2×2 mm2) area and (ii) FET with a single gate and ohmic contacts forming a bow-tie antenna. By raster scanning the detector area by using a tightly focused terahertz beam, we studied the contribution of individual parts of the detector to the total detection response and we determined the effective area of the detector structures.

1. Introduction

Up to date, a number of terahertz (THz) plasmonic detectors based on the FET structures have been proposed and investigated [1]-[4]. Most studies have been performed with using the experimental setup where the size of the detector was smaller than the size of the cross section of THz beam. In such experiments, the important question of an effective area of the detector in terms of the detector responsivity and its coupling strength to incident THz radiation could not be experimentally analyzed.

In the present study were investigate two conceptually different THz plasmonic detectors: (i) FET with a single gate and a broadband bow-tie antenna and (ii), the FET structure with a grating-gate of large area.

2. Sample fabrication and measurements

A material system for the devices is an AlGaAs/InGaAs/GaAs heterostructure (see [2]) grown by the molecular beam epitaxy. The top view of grating-gate and bow-tie detectors is shown in figure 1. The microchip holder with the detector was mounted on the translation stage which could move in three dimensions. A continuous source of linearly polarized THz radiation was a gas laser SIFIR-50. The operation parameters of the THz laser are listed in the table 1.

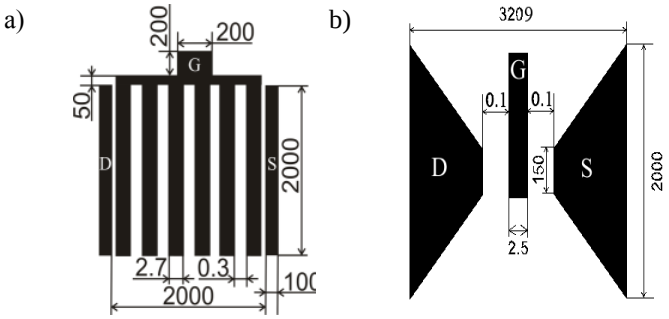

Figure 1. Top view of the investigated detectors (all dimensions are given in microns): a) grating-gate detector; b) bow-tie detector.

Table 1. Operation parameters of THz source.

f, THz	1.63	1.89	2.55
λ, μm	184	159	118
Sspot, mm2	0.027	0.020	0.011
P, mW	143.1	86.6	108.8

In table 1, the following designations are used: f is the operation frequency, λ is the wavelength of THz radiation, S_{spot} is the minimum area of the THz beam spot, $S_{pot}=\pi\times(\lambda/2)^2$, and P is the THz power.

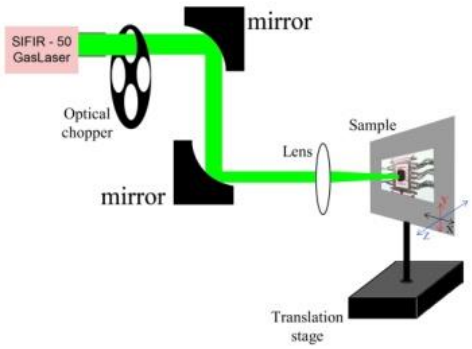

Figure 2. Measurement setup.

Terahertz radiation was chopped at frequency of about 100 Hz, and then, through the focusing optical system, was impinged onto the sample. The radiation beam was focused to a spot with a diameter about the wavelength of the incident radiation by means of parabolic mirrors (figure 2). This allowed us to scan the area of the wide-aperture detector. All measurements were performed at room temperature. Photoresponse signal was measured using a standard lock-in detection technique.

3. Results and discussion

3.1. Bow-tie detector

Raster scans for the bow-tie plasmonic detector at frequencies 1.63 and 2.55 THz are shown in figure 3.

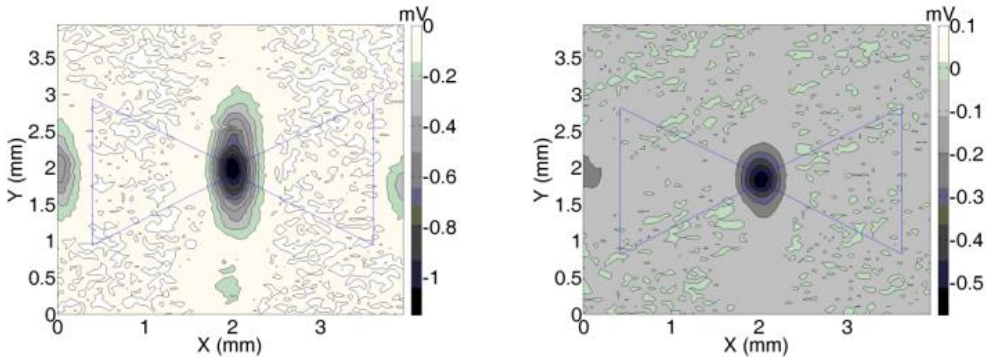

(a) (b)

Figure 3. Raster scans images of the THz photoresponse for the bow-tie plasmonic detector at frequencies (a) 1.63 and (b) 2.55 THz for the drain current $I_d = 25$ μA, gate voltage $V_g = -40$ mV, and the leakage current $I_g = -1.65$ nA. The position of the detector is also schematically shown.

It follows from the raster scan images that the effective detection area is 0.11 and 0.07 mm^2 for 1.63 and 2.55 THz, respectively, with respective responsivities 0.19 V/W and 0.22 V/W. Responsivity, *R*, was calculated by the formula

$$R = \frac{\iint_{image} PhResp \times dxdy}{P \times S_{spot}}, \quad (1)$$

where PhResp is the photoresponse. Double integral is calculated over the image area. The effective image area is calculated at $1/\sqrt{2}$ of the maximum photoresponse in the raster scan image.

3.2. Grating-gate detector

Previously, the grating-gate FET detector was examined for resonance detection of sub-THz radiation in [2], [4]. In those studies, incident THz radiation was uniformly distributed over the area of the sample (the cross-section area of THz beam exceeded the sample area). However, due to possible non-uniformity of a large-area grating-gate structure, different parts on the structure might contribute differently to the overall THz detection response. Scanning the device area by a narrow THz beam, allows us to detect the effective area of THz detection.

Raster scan THz images of the grating-gate detector measured at frequency 1.89 THz for zero drain bias current are shown in figures 4 and 5. Due to the symmetry of the grating gate, there is no detection contribution from the grating area of the structure. It can be seen in figure 4 that the detection contributions from the source and drain contacts, being almost of the value, are of opposite signs. Because of that the contact contributions effectively cancel each other and hence do not virtually affect the overall THz photoresponse. The raster scan THz images of the grating-gate detector for different values of the drain bias current are shown in figure 5.

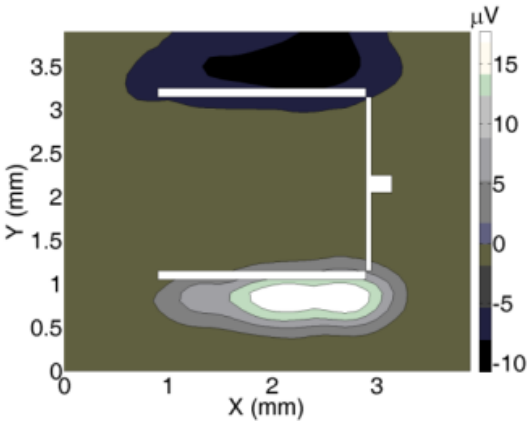

Figure 4. Raster scan images of THz photoresponse of the grating-gate detector for zero gate voltage and $I_d = 0$. The position of the detector is also schematically shown.

Detector responsivities calculated by Eq. (1) are 29, 72, 94, and 155 mV/W for figures from 5a to 5d, respectively. The value of THz photoresponse increases with increasing the bias current. However, the THz photoresponse from the grating-gate area is exhibited even for zero drain bias current (see figure 5c). This can be attributed to a relatively strong gate-leakage current I_g flowing in the channel even for vanishing drain current. Because the leakage current flowing in the source-gate circuit [5] is unidirectional, the photoresponse is different for opposite polarities of the drain bias current (cf. figures 5a and 5d).

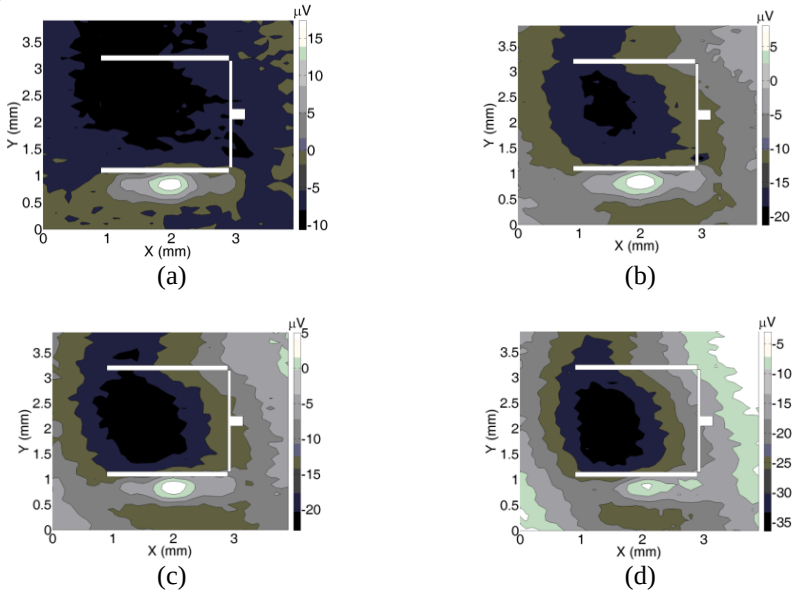

Figure 5. Raster scan images of THz photoresponse of the grating-gate detector for the gate voltage –1 V: a) $I_d = 448$ μA, $I_g = 607$ μA; b) $I_d = 170$ μA, $I_g = 481$ μA; c) $I_d = 0$, $I_g = 412$ μA ; d) $I_d = –448$ μA, $I_g = 268$ μA. The position of the detector is also schematically shown.

It is seen in figure 5 that the effective area of detection is 3.2 mm^2, which is about 80% of the total area of the grating-gate. The decrease in the effective area of the detector is due to the shunting of the THz electric field by the metal bus lead connecting the grating-gate fingers (right white line of the

grating-gate contour in figures 5 a-d). This lead affects the distribution of the external incident field over the distance of $2\times\lambda=0.318$ mm from the lead, thereby reducing the effective detection area by 16%. This value is in good correspondence with the measured effective area of the detector (20%). Since the almost entire area of the grating gate along its periodicity retains its effectiveness, it can be concluded that the majority of the grating-gate fingers work effectively.

4. Conclusions

We report on an experimental investigation of the wide-aperture THz plasmonic detectors by using a tightly focused THz beam. This study allows for direct measurement of the effective area of the detector that provides opportunities for further improving the design of large-aperture detectors and can be used for analyzing the coupling efficiency between the detector and THz radiation. This analysis can also form the basis for the development of the quality control of multi-gated FET structures.

Acknowledgement

This work was partly supported by the RAS Programs "Fundamentals and Technological Development of the Nanoelectronic and Nanostructure Sensor Components in the Microwave and Terahertz Ranges" and "Fundamentals of Nanostructure Technologies and Nanomaterials."

References

[1] Peralta X G, Allen S J , Wanke M C, Harff N E, Simmons J A, Lilly M P, Reno J L, Burke P J, and Eisenstein J P 2002 *Appl.Phys. Lett.* **81** 1627
[2] Yermolaev D M, Marem'yanin K M, Fateev D V, Morozov S V, Maleev N A, Zemlyakov V E, Gavrilenko V I, Shapoval S Yu, Sizov F F and Popov V V 2013 *Solid-State Electron.* **86** 64
[3] Lisauskas A, Pfeiffer U,Öjefors E, Haring Bolìvar P, Glaab D and Roskos H G 2009 *J. Appl. Phys.* **105** 114511
[4] Marem'yanin K V, Ermolaev D M, Fateev D V, Morozov S V, Maleev N A, Zemlyakov V E, Gavrilenko V I, Popov V V, and Shapoval S Yu 2010 *Techn.Phys.Lett.* **36**(4) 365
[5] Dyakonov M and Shur M 1993 *Phys.Rev.Lett.* **71** 15